

# DISSIPATION ELEMENT ANALYSIS OF SCALAR FIELDS IN WALL-BOUNDED TURBULENT FLOW

**Fettah Aldudak**

Chair of Fluid Dynamics, Department of Mechanical Engineering, TU Darmstadt,  
Petersenstr. 30, 64287 Darmstadt, Germany  
aldudak@fdy.tu-darmstadt.de

**Martin Oberlack**

Chair of Fluid Dynamics, Department of Mechanical Engineering, TU Darmstadt,  
Petersenstr. 30, 64287 Darmstadt, Germany  
Center of Smart Interfaces, TU Darmstadt, Petersenstr. 32, 64287 Darmstadt, Germany  
GS Computational Engineering, TU Darmstadt Dolivostr. 15, 64293 Darmstadt, Germany  
oberlack@fdy.tu-darmstadt.de

## ABSTRACT

The scalar fields obtained by Direct Numerical Simulations (DNS) are decomposed into numerous finite size regions using the dissipation element analysis proposed by Wang & Peters (2006) providing detailed information about the geometry of turbulent structures - presently for the turbulent channel flow. Therefore local pairs of minimal and maximal points in the scalar field  $\phi(x, y, z, t)$  are detected where  $\nabla\phi = 0$ . Gradient trajectories of finite length starting from every point in the scalar field in the directions of ascending and descending scalar gradients will reach a minimum and a maximum point with  $\nabla\phi = 0$ . The set of all points belonging to the same pair of extremal points defines a dissipation element (DE). Hence, the decomposition of the domain into dissipation elements is not arbitrary but follows from the structures of the flow itself and further is completely space filling. The components of the velocity, the vorticity vector, the kinetic energy and its dissipation could be chosen as such a scalar field  $\phi$ . The Euclidian distance  $\ell$  between the extremal points and the absolute value of the scalar difference  $\Delta\phi$  at these two points mark the key parameters to parameterize the geometry and the field variable structure of the dissipation elements. Although these spatial structures are irregularly shaped the parameters mentioned give a deep insight into the length scale and scalar increment distribution (Wang & Peters (2006)). For the case of homogeneous shear turbulence the authors in Wang & Peters (2006) report that the mean DE length is in the order of the Taylor scale defined as  $\lambda = (10\nu k/\varepsilon)^{1/2}$ . This can be confirmed presently for the turbulent channel flow though it is a statistically inhomogeneous flow in the wall-normal direction  $y$ .

## DNS of turbulent channel flow

Wall-bounded turbulent channel flow features some characteristic wall-normal layers namely, viscous sublayer, buffer

layer, logarithmic region and the core/defect region. Corresponding to the respective layers different turbulence phenomena are dominant leading to inhomogeneity in all wall-normal statistics. This typically applies to the turbulent length scales as well. While sufficiently far from the wall large scale length scales ( $\ell \gg \eta$ ) are widely independent of the influence of viscous forces the latter become very influential approaching the wall. The anisotropic largest turbulent scales correspond to the integral length scale which are of the order of channel height.

A spectral numerical method using Fourier series in the horizontal streamwise ( $x$ ) and spanwise ( $z$ ) directions and Chebyshev polynomial expansion in the wall-normal ( $y$ ) direction is applied to solve the three-dimensional time-dependent incompressible Navier-Stokes equations in the dimensionless form (for details see Lundbladh *et al.* (1999))

$$\frac{\partial \mathbf{u}}{\partial t} + (\mathbf{u} \cdot \nabla) \mathbf{u} = -\nabla p + \frac{1}{Re_\tau} \nabla^2 \mathbf{u}, \quad (1)$$

$$\nabla \cdot \mathbf{u} = 0, \quad (2)$$

where  $\mathbf{x}$ ,  $t$ ,  $\mathbf{u}$  and  $p$  are respectively the position vector, time, the velocity vector and pressure. Time integration is performed using a third order Runge-Kutta scheme for the advective and forcing terms and second order Crank-Nicolson for the viscous terms. While periodic boundary conditions are applied in the homogeneous streamwise ( $x$ ) and spanwise ( $z$ ) directions no-slip boundary condition is adopted at the channel walls where  $\mathbf{u}(x, y=\pm 1, z) = 0$ .  $\mathbf{u} = (u, v, w)$  denote the streamwise, wall-normal and spanwise velocity components.

Presently, the channel flow at two Reynolds numbers  $Re_\tau = u_\tau h/\nu$  are analyzed, where  $u_\tau = \sqrt{\tau/\rho}$  is the friction

velocity,  $\tau$  is the mean wall-shear stress and  $\rho$  is the density (see table 1). The numerical resolution  $N_x \times N_y \times N_z$  reads  $512 \times 257 \times 256$ .

Table 1. Simulation parameters.  $h$  denotes the channel half-height.

-	$Re_\tau$	$L_x/h$	$L_z/h$
Case 1	180	$2\pi$	$\pi$
Case 2	360	$2\pi$	$\pi$

### Dissipation Element statistics

The probability density function (*pdf*) depending on the Euclidian length  $\ell$ , the conditional mean scalar difference  $\langle \Delta\phi | \ell \rangle$ , and in particular its dependence on the wall distance  $y$ , describing each element will be the main focus of the present work. The *pdf* states the distribution of the element lengths and the latter shows the scaling behavior of the scalar difference with respect to the length. Hence, rather generally, the present *pdf* is a function with the dependencies  $P(\ell, \Delta\phi, y, Re_\tau)$  satisfying the normalization condition

$$\int_0^\infty P d\ell = 1. \quad (3)$$

The mean or expectation value for the DE length is defined as

$$\ell_m = \int_0^\infty \ell P d\ell. \quad (4)$$

For the analysis of DE we investigate three scalar field variables, the fluctuation of the streamwise velocity component  $u$ , the turbulent kinetic energy  $k$  and its dissipation rate  $\varepsilon$ , which is highly intermittent, at two Reynolds numbers being a factor of two apart. The latter two are defined as

$$k = \frac{1}{2} (u^2 + v^2 + w^2), \quad (5)$$

$$\varepsilon = \frac{1}{2} \nu \left( \frac{\partial u_i}{\partial x_j} + \frac{\partial u_j}{\partial x_i} \right)^2, \quad (6)$$

where  $\nu$  is the kinematic viscosity.

The figures in 1 illustrate the dependence of the marginal pdf of the Euclidian DE length on (a) Reynolds number and (b) different scalar variables. Here,  $\tilde{P} = \ell_m P$  and  $\tilde{\ell} = \frac{\ell}{\ell_m}$  are invariants where  $\ell_m$  is the mean DE length defined in equation (4). All pdf feature a clearly non-Gaussian distribution. For

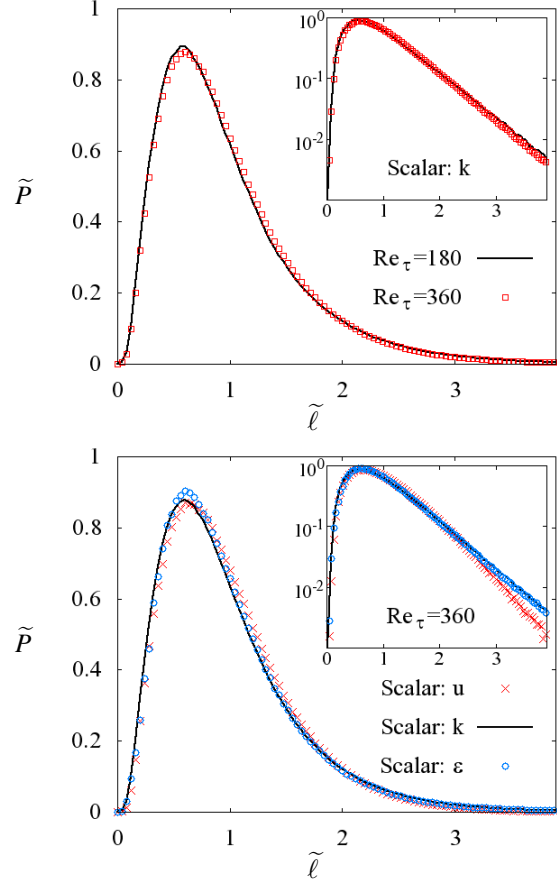


Figure 1. Comparison of the overall *pdf* of the entire channel for different (a) Reynolds numbers and (b) scalar variables.

small DE the curves show a very steep rise before reaching a maximum at around  $\ell \approx 0.6\ell_m$  marking the highest probability for DE length scales. With further increasing DE length an exponential decay becomes evident which can be seen even better in the small inset figures. Figure 1 (a) reveals a very interesting insensitivity with respect to Reynolds number for the scalar of  $k$  as an example. Despite the relatively big gap between both  $Re$  their pdf coincide almost perfectly. The same conclusion applies to the dependency regarding to the choice of the scalar variable as can be observed in figure 1 (b). All three curves exhibit a very good agreement with each other almost throughout the entire spectrum of DE length scales. Only around the maximum and in the far-tail of the pdf one can see small deviations.

At this point pdf for  $k$  and  $\varepsilon$  seem to be closer than the velocity component  $u$  which decays faster as displayed in the semi-logarithmic illustration. Nevertheless, the obvious insensitivity with respect to the choice of the scalar variable implies a pronounced DE isotropy for all DE spectrum.

In figure 2 (a) the linear length of DE averaged over the horizontal directions  $x, z$  is plotted as a function of the wall-normal direction from the wall ( $y/h = 0$ ) up to the centerline of the channel ( $y/h = 1$ ) again for the three scalar variables. All curves display a characteristic linear behavior in the same wall-normal region. This means that DE size grows linearly

in this region such as

$$\ell_m \sim y + c. \quad (7)$$

This relation applies to the region  $0.2 \leq y/h \leq 0.8$  which consists of the logarithmic layer and most of the defect layer only excluding the viscosity dominated near-wall layer and the very center region (central core). Above this, DE size appears to remain constant in the center of the channel which might be due to the low shear occurring here. This is more obvious for  $u$  and  $k$  but applies to  $\varepsilon$  as well. On the contrary, no clear tendency can be detected for the near-wall region including viscous and buffer regions.

Additionally, one recognizes the differences with respect to the mean DE length for different scalar variables. This is due to the different number of extremal points that are created by turbulence which of course depends on the choice of the scalar. Since the DE length is defined by the distance of the corresponding minimum and maximum points the size of DE will be smaller on average if the number of the points increases. Accordingly, picture 2 (a) shows that for the scalar variables considered here the  $\varepsilon$  field features the smallest elements indicating a higher number of extremal points, which has been evaluated (not shown here), followed by  $k$  and  $u$ . Given the fact that, unlike classical turbulent length scales, DE are space filling, hence, occupy the whole flow field the number of DE must decrease towards the center of the channel due to the increase of the element size (see equation (7)).

In figure 2 (b) the relation between the DE and the Taylor length scales  $\ell_m/\lambda$  as a function of  $y/h$  is highlighted exposing that for a wide range of wall-normal direction  $\ell_m$  scales excellent with the Taylor length scale  $\lambda$ , in other words

$$\ell_m \sim \lambda. \quad (8)$$

For reasons mentioned above the proportionality constant varies depending on the scalar variable, i.e.  $\ell_m \approx \lambda$  for  $\varepsilon$ ,  $\ell_m \approx 2\lambda$  for  $k$  and  $\ell_m \approx 3\lambda$  for  $u$ . Whereas this relationship holds true even for the channel center it is clearly broken near the wall.

In figures 3 pdf of DE length have been investigated for three characteristic wall-normal layers of a turbulent channel flow exemplarily for the case of  $k$  to explore the influence of the distance from the wall. The very thin viscous sublayer has been excluded to avoid ambiguity of the DE definition at the wall. The layers defined in terms of the wall distance are as follows.

$$\begin{aligned} \text{buffer region: } & 5 < y^+ < 30 \\ \text{log region: } & y^+ \geq 30, y/h < 0.3 \\ \text{core region: } & 0.3 \geq y/h < 1 \end{aligned}$$

where  $y^+ = yu_\tau/\nu$ .

The pdf in figure 3 (a) are normalized only according to equation (3) while in figure 3 (b) the length scale has also been normalized by the corresponding local mean length  $\ell_m$  of the channel layer. As can be seen, without re-scaling of the pdf figure 3 (a) features huge deviations indicating a strong

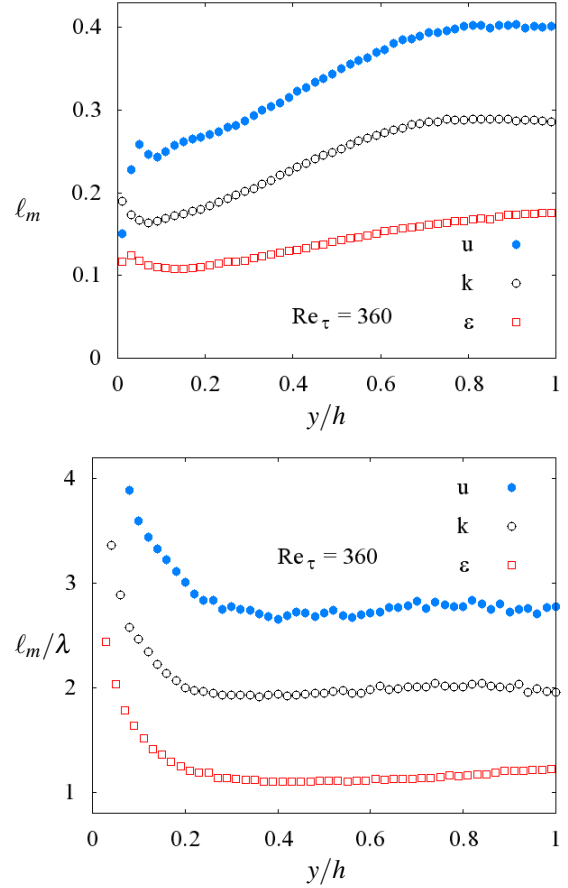


Figure 2. (a) Mean DE length along wall-normal direction. (b) Mean DE length normalized by the Taylor length scale  $\lambda$ .

impact of the wall distance on the pdf. The pdf closer to the wall exhibit a narrower shape while at the same time the maximum peak moves towards smaller element lengths. Thus, one can conclude that smaller elements can be encountered near the wall whereas larger elements are mostly located in the far-wall regions. This is in agreement with the observations on the basis of figure 2 where the DE length distribution illustrates the influence of the wall distance. Furthermore, with its broader shape pdf for the core region reveals that this layer consists of a wider spectrum of length scales than the logarithmic and the buffer regions.

On the other hand, the pdf curves exhibit an evident similarity if  $\ell$  is normalized with the according mean length, i.e.  $\tilde{\ell} = \ell/\ell_m$ . Thus, the rescaled similarity variable  $\tilde{P} = \ell_m P$  is plotted in figure 3 (b). An almost complete collapse of the pdf is displayed for the logarithmic and the core regions which together amount to more than 90% of the entire channel. In contrast, pdf for the near-wall buffer region is substantially different from others as a result of predominant wall and viscous effects. The lack of linear scaling of the mean DE length in the buffer layer which was observed in the far-wall regions is certainly the reason for this deviation.

In the next step we analyze the conditional mean scalar differences between the values at the extremal points conditioned on the length of the corresponding dissipation ele-

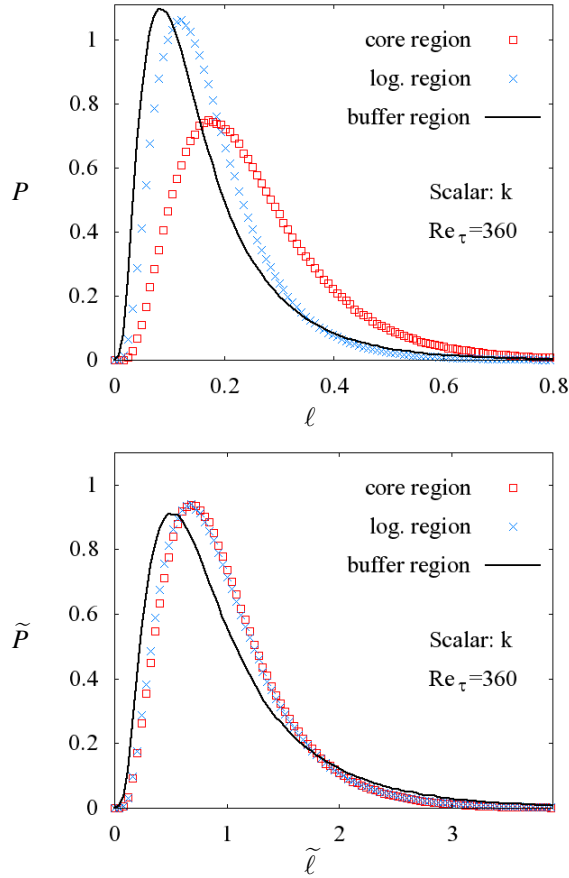


Figure 3. pdf for characteristic wall-normal layers where in (a)  $\ell$  is not normalized while in (b)  $\ell$  is normalized with  $\ell_m$ .

ment for the instantaneous turbulent kinetic energy  $k$ . Therefore, the first order conditional moment is investigated to measure its scaling along wall-normal distance. The first moment based on gradient trajectories is non-zero since the value of the turbulent kinetic energy increases per definition monotonically along a trajectory from the minimum to the maximum point.

Hence, in figure 4 conditional mean scalar difference is plotted for different wall-normal layers. In (a) we focus on a restricted region in the very center region (central core) corresponding to  $0.8 \leq y/h \leq 1$  featuring the highest degree of isotropy and the weakest shear in present flow regime. For sufficiently large DE the logarithmic plot reveals a scaling exponent of  $2/3$  which is known from Kolmogorov's law. Approaching the wall, of course, this scaling is likely to break under the influence of shear induced anisotropy as can be confirmed by the semi-logarithmic plots. In the near-wall buffer layer and the logarithmic layer where turbulent kinetic energy scales as  $u_z^2$  we observe a  $\ln(\ell)$  law equivalent to the classical  $K^{-1}$  law (Perry *et al.* (1986)). In the buffer layer this behavior is extended to an even wider spectrum of elements.

## Conclusion

We applied the Dissipation Element (DE) method to the wall-bounded turbulent channel flow to analyze its geometri-

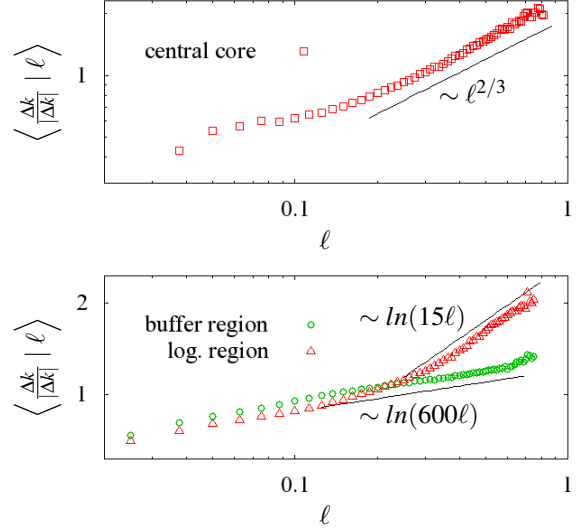


Figure 4. Conditional mean scalar differences for different wall-normal channel layers. (a) logarithmic, (b) semi-logarithmic.

cal structure. Different statistics such as the probability density function (pdf) for different turbulent scalar variables, the conditional mean scalar difference of the turbulent kinetic energy and the DE length have been subject of the present work. The dependency of this statistics on the wall-normal distance in terms of characteristic wall-normal regions (buffer, logarithmic and core regions) has been investigated. Generally, strong influence of the wall could be observed in all statistics except for rescaled pdf for different channel layers yielding invariant forms of the pdf. Mean DE size was found to have clear linear scaling with respect to the distance from the wall as well as the conditional mean scalar differences between the extremal points of DE. For the latter, it could be shown that in the very center of the channel Kolmogorov's  $2/3$  scaling holds whereas layers closer to wall feature a logarithmic law rather than a power law. As future prospects we aim to extend our findings to higher Reynolds numbers and to more scalar variables to serve a more complete picture of the geometrical structure of turbulence.

## REFERENCES

- Lundbladh, A., Berlin, S., Skote, M., Hildings, C., Choi, J., Kim, J. & Henningson, D. S. 1999 An efficient spectral method for simulation of incompressible flow over a flat plate. Technical Report 1999:11. KTH, Stockholm.
- Perry, A. E., Henbest, S. M. & Chong, M. S. 1986 A theoretical and experimental study of wall turbulence. *J. Fluid Mech.* **163**, 163–199.
- Wang, L. & Peters, N. 2006 The length scale distribution function of the distance between extremal points in passive scalar turbulence. *J. Fluid Mech.* **554**, 457–475.